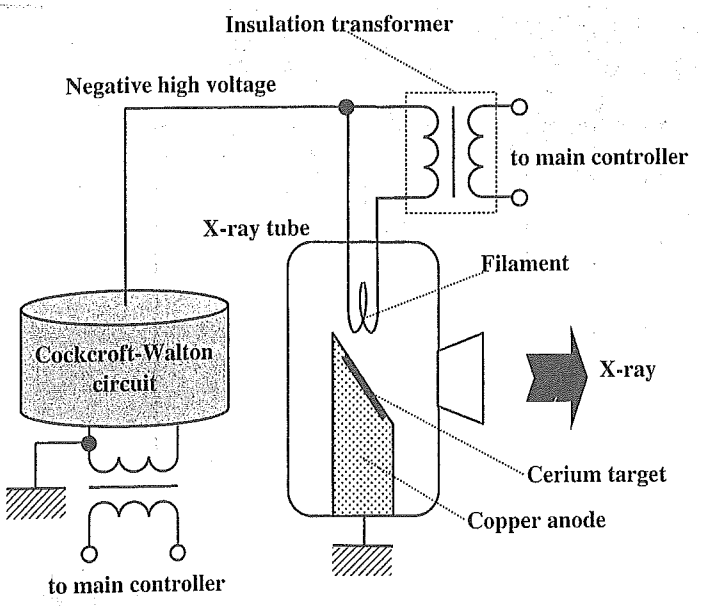


Fig. 2. Main circuit of X-ray generator.

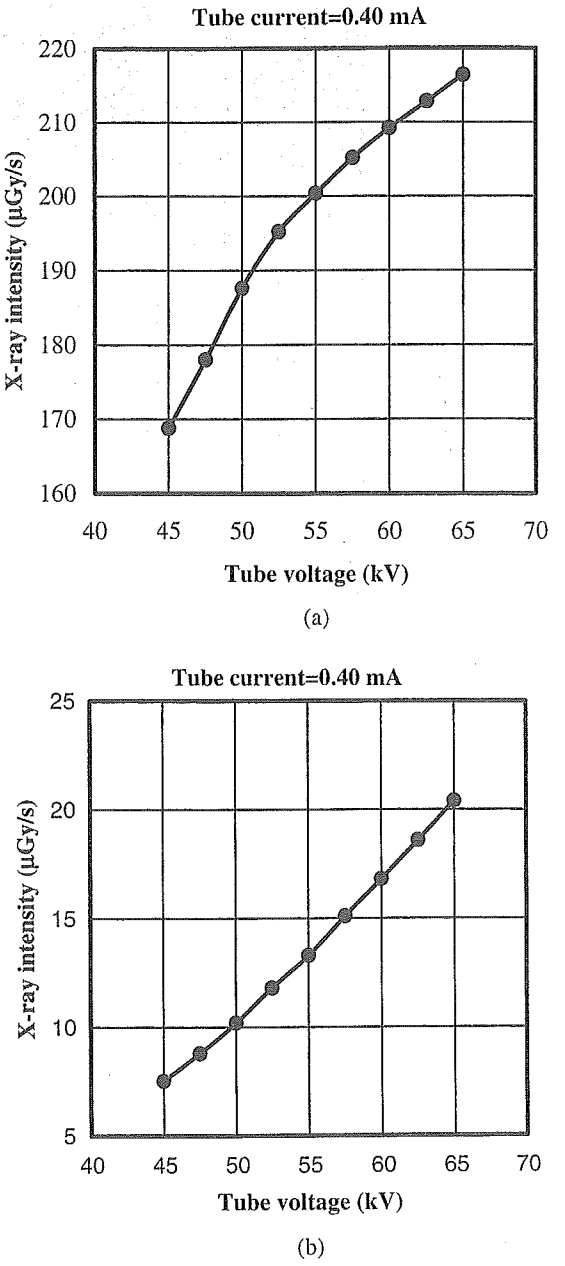


Fig. 3. X-ray intensity measured at 1.0 m from X-ray source according changes in tube voltage (a) without filtering and (b) using barium-sulfa filter.

with a Cockcroft–Walton circuit and a cerium-target tube. The tube voltage, the current, and the exposure time can be controlled by the controller. The main circuit for producing X-rays is illustrated in Fig. 2, and it employed the Cockcroft–Walton circuit in order to decrease the dimensions of the tube unit. In the X-ray tube, a high negative voltage is applied to the cathode electrode, and the anode (target) is connected to the tube unit case (ground potential) to cool the anode and the target effectively. The filament heating current is supplied by an AC power supply in the controller in conjunction with an insulation transformer. The tube is a conventional diode with a plate cerium target, a 1.0 mm focus, a take-off angle of 22°, and a 0.5-mm-thick beryllium window. In this experiment, the tube voltage was from 45 to 65 kV, and the tube current was regulated to within 0.40 mA (maximum current) by the filament temperature. The exposure time is controlled in order to obtain optimum X-ray intensity. Monochromatic K$\alpha$ rays are selected out using a barium sulfate filter for absorbing bremsstrahlung and K$\beta$ rays. In designing the filter, the surface density of the barium sulfate powder is important, since the X-rays are absorbed effectively by the powder as compared with poly(methyl methacrylate) (PMMA) resin. In this case, the density was approximately 30 mg/cm$^2$.

## 3. Characteristics

### *3.1 X-ray intensity*

The X-ray intensity rate was measured by a Victoreen 660 ionization chamber at 1.0 m from the X-ray source (Fig. 3). At a constant tube current of 0.40 mA, the X-ray intensity increased when the tube voltage was increased. At a tube voltage of 60 kV and a current of 0.40 mA, the intensities without filtering and with the filter were 208 and 16.8 μGy/s, respectively, with errors of less than 0.2%. The X-ray intensity was limited because the thermal contact between the target and the anode was not good.

### *3.2 X-ray spectra*

In order to measure X-ray spectra, we employed a germanium detector (GLP-10180/07-P, Ortec Inc.) (Fig. 4 Without filtering, when the tube voltage was increased, th X-ray intensities of cerium K-series characteristic line increased, and both the maximum photon energy and th bremsstrahlung X-ray intensity increased. Using the filte both the K$\beta$ lines and the bremsstrahlung X-rays with photo energies higher than the barium K-edge of 37.4 keV wer absorbed effectively, and sharp K$\alpha$ lines were left. Wit increases in the tube voltage, the K$\alpha$ intensity substantiall increased, and the maximum photon energy increased.

In order to perform K-edge angiography, the K$\alpha$ rays ar useful, and the high-energy bremsstrahlung X-rays decreas the image contrast. Using the filter, because bremsstrahlun X-rays with energies higher than 60 keV were not absorbe easily, the tube voltage for angiography was determined t be 60 kV. Subsequently, low-energy bremsstrahlung ray

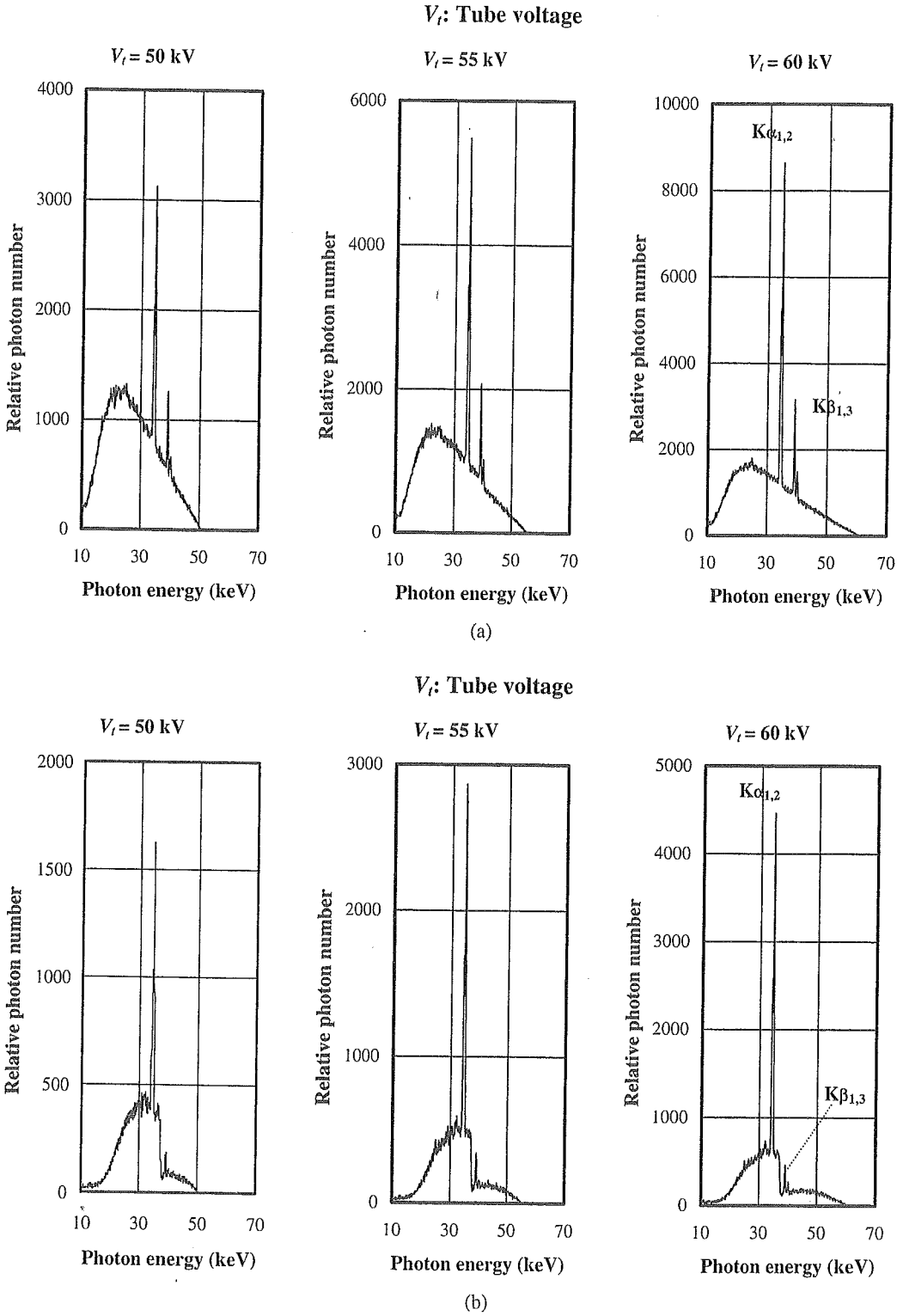


Fig. 4. X-ray spectra measured using germanium detector with changes in tube voltage (a) without filtering and (b) using barium sulfate filter.

with energies lower than the K-edge should be minimized using the filter or an aluminum filter to increase the blood-vessel contrast, since the iodine contrast media transmit the rays easily.

## 4. K-edge Angiography

Because the average photon energy of K$\alpha$ is 34.6 keV, iodine contrast media with a K-absorption edge of 33.2 keV absorb the K$\alpha$ lines easily. Therefore, blood vessels were observed with high contrasts. In order to observe fine blood vessels approximately 50 μm in diameter, the angiography was performed using an X-ray film (Fuji IX 100), iodine microspheres 15 μm in diameter, and the filter. The distance between the X-ray source and the imaging plate was 1.5 m, and the tube voltage was 60 kV. First, rough measurements of spatial resolution were made using wires. Figure 5 shows radiograms of tungsten wires coiled around rods made of PMMA with an X-ray exposure time of 300 s. Although the

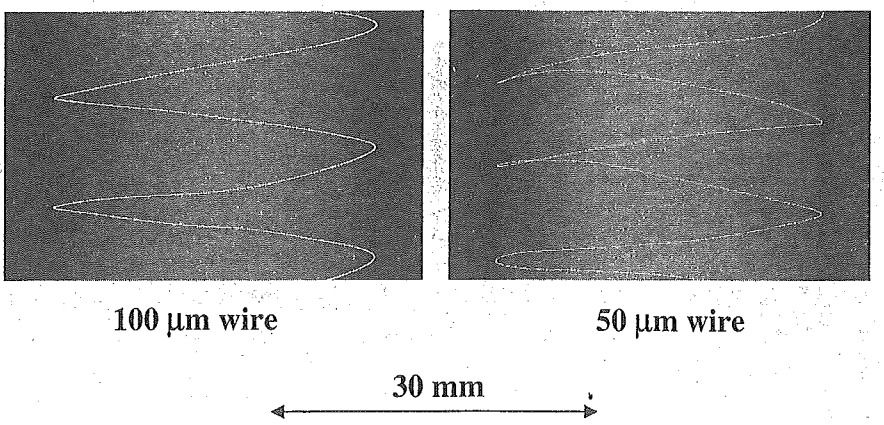


Fig. 5. Radiograms of tungsten wires coiled around PMMA rods.

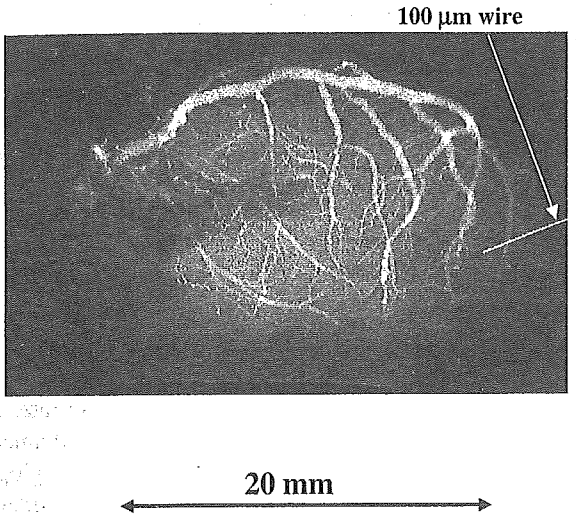


Fig. 6. Angiograms of extracted rabbit heart using iodine microspheres.

image contrast hardly varied with decreases in the wire diameter, a 50-μm-diameter wire could be observed clearly.

Figures 6 and 7 show angiograms of a rabbit heart and a thigh, respectively, with an exposure time of 300 s. The coronary arteries in the heart and fine blood vessels in the thigh with diameters of approximately 100 μm were visible. Figure 8 shows an angiogram of a dog heart in a 100-mm-thick water phantom with an exposure time of 1,500 s. Because the size of the dog heart is almost the same as that of a human heart, human coronary arteries can be observed. For comparison, we show a three-dimensional (3D) image of the coronary arteries constructed from X-ray CT images taken by Pascal (Digital Culture Tech. Corp.) with a tungsten X-ray tube (Fig. 9). This heart was the same as that used in K-edge angiography and was observed from the same direction by rotating the three-dimensional (3D) image; CT angiography was performed without using the water phantom. Using this 3D angiography achieved with a multislice helical CT, fine blood vessels were not observed at all.

## 5. Discussion

In the present research, we employed an X-ray generator with a cerium-target tube and succeeded in producing cerium characteristic X-rays, which can be absorbed easily by iodine-based contrast media. Both the characteristic and bremsstrahlung X-ray intensities increased with tube voltage

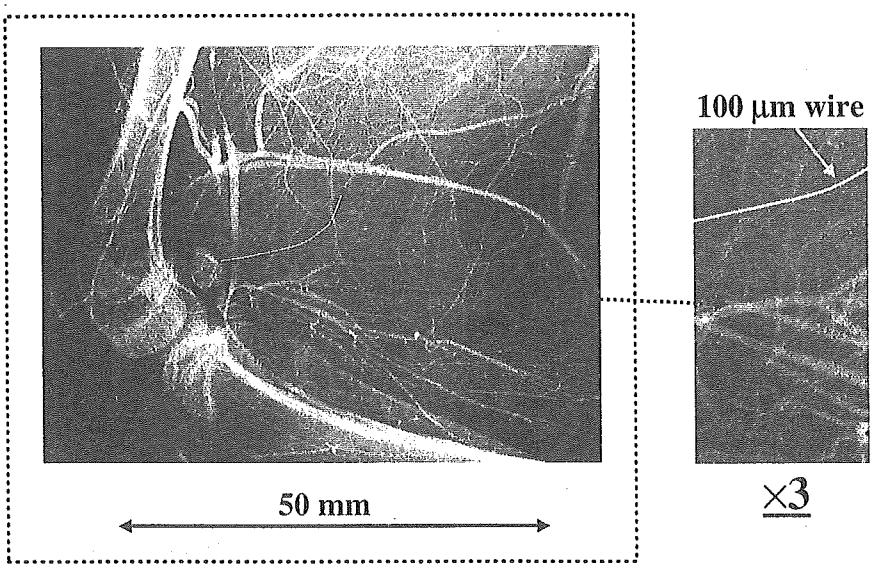


Fig. 7. Angiogram of rabbit thigh using iodine microspheres.

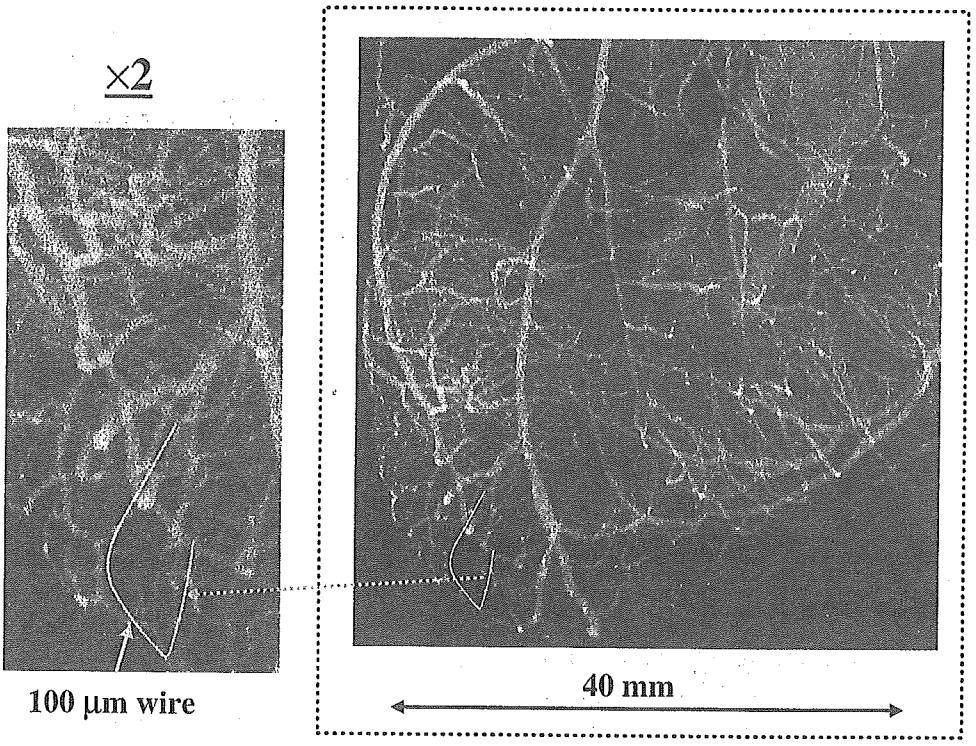


Fig. 8. Angiogram of extracted dog heart in 100-mm-thick water phantom using iodine microspheres.

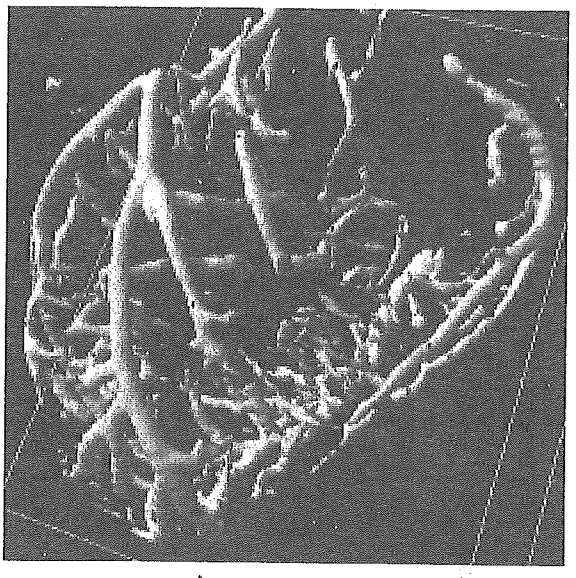

Fig. 9. Three-dimensional image of coronary arteries constructed from X-ray CT images taken by Pascal.

without filtering. Using the filter to absorb K$\beta$ and bremsstrahlung X-rays, K$\alpha$ rays were left, and we performed K-edge angiography using the filter with a tube voltage of 60 kV. To produce clean characteristic X-rays without using the filter, the angle dependence of the bremsstrahlung intensity should be considered, since bremsstrahlung rays are not emitted in the direction opposite that of the electron trajectory in Sommerfeld's theory.[18)]

Currently, angiography is performed using both the bremsstrahlung and characteristic X-rays produced from a tungsten X-ray tube. However, enhanced K-edge angiography in this work was primarily performed using cerium K$\alpha$ rays. Using the filter, the maximum number of K$\alpha$ photons was approximately $3 \times 10^7$ photons/(cm$^2$·s) at 1.0 m from the source, and the photon count rate can be increased easily by improving the target. For example, a new rotation anode tube has been designed to increase the X-ray dose rate, and the rate can be increased by increasing the anode diameter.

In energy-selective imaging including K-edge angiography, the filtering effect of the absorber should be considered, and the X-ray spectra using the filter at a tube voltage of 60 kV hardly varies with changes in the thickness of the water phantom according to the spectrum estimation. Due to the absorption coefficient, K$\beta$ rays are also useful for angiography, and both the K$\alpha$ and K$\beta$ rays can be left using a cerium oxide filter with a surface density of approximately 10 mg/cm$^2$. In addition, an aluminum filter with a thickness of approximately 3.0 mm is useful in absorbing unnecessary bremsstrahlung X-rays with energies lower than the K-absorption edge.

## Acknowledgment

This work was supported by Grants-in-Aid for Scientific Research (13470154, 13877114, 16591181, and 16591222) and Advanced Medical Scientific Research from MECSST, Health and Labor Sciences Research Grants (RAMT-nano-001, RHGTEFB-genome-005 and RHGTEFB-saisei-003), Grants from the Keiryo Research Foundation, The Promotion and Mutual Aid Corporation for Private Schools of Japan, Japan Science and Technology Agency (JST), and the New Energy and Industrial Technology Development Organization (NEDO, Industrial Technology Research Grant Program in '03).

1) A. Akisada, M. Ando, K. Hyodo, S. Hasegawa, K. Konishi, K. Nishimura, A. Maruhashi, F. Toyofuku, A. Suwa and K. Kohra: Nucl. Instrum. Methods Phys. Res., Sect. A **246** (1986) 713.
2) A. C. Thompson, H. D. Zeman, G. S. Brown, J. Morrison, P. Reiser,

V. Padmanabahn, L. Ong, S. Green, J. Giacomini, H. Gordon and E. Rubenstein: Rev. Sci. Instrum. **63** (1992) 625.
3) H. Mori *et al.*: Radiology **201** (1996) 173.
4) K. Hyodo, M. Ando, Y. Oku, S. Yamamoto, T. Takeda, Y. Itai, S. Ohtsuka, Y. Sugishita and J. Tada: J. Synchrotron Radiat. **5** (1998) 1123.
5) T. J. Davis, D. Gao, T. E. Gureyev, A. W. Stevenson and S. W. Wilkims: Nature **373** (1995) 595.
6) A. Momose, T. Takeda, Y. Itai and K. Hirano: Nat. Med. **2** (1996) 473.
7) M. Ando, A. Maksimenko, H. Sugiyama, W. Pattanasiriwisawa, K. Hyodo and C. Uyama: Jpn. J. Appl. Phys. **41** (2002) L1016.
8) E. Sato, S. Kimura, S. Kawasaki, H. Isobe, K. Takahashi, Y. Tamakawa and T. Yanagisawa: Rev. Sci. Instrum. **61** (1990) 2343.
9) A. Shikoda, E. Sato, M. Sagae, T. Oizumi, Y. Tamakawa and T. Yanagisawa: Rev. Sci. Instrum. **65** (1994) 850.
10) K. Takahashi, E. Sato, M. Sagae, T. Oizumi, Y. Tamakawa and T. Yanagisawa: Jpn. J. Appl. Phys. **33** (1994) 4146.
11) E. Sato, K. Takahashi, M. Sagae, S. Kimura, T. Oizumi, Y. Hayasi, Y. Tamakawa and T. Yanagisawa: Med. Biol. Eng. Comput. **32** (1994) 289.
12) E. Sato, Y. Hayasi, R. Germer, E. Tanaka, H. Mori, T. Kawai, T. Ichimaru, K. Takayama and H. Ido: Rev. Sci. Instrum. **74** (2003) 5236.
13) E. Sato, Y. Hayasi, R. Germer, E. Tanaka, H. Mori, T. Kawai, T. Ichimaru, S. Sato, K. Takayama and H. Ido: J. Electron Spectrosc. Relat. Phenom. C **137–140** (2004) 713.
14) E. Sato, Y. Hayasi, R. Germer, E. Tanaka, H. Mori, T. Kawai, H. Obara, T. Ichimaru, K. Takayama and H. Ido: Jpn. J. Med. Phys. **20** (2003) 123.
15) E. Sato, E. Tanaka, H. Mori, T. Kawai, T. Ichimaru, S. Sato, K. Takayama and H. Ido: Med. Phys. **32** (2005) 49.
16) E. Sato, E. Tanaka, H. Mori, T. Kawai, T. Ichimaru, S. Sato, K. Takayama and H. Ido: Med. Phys. **31** (2004) 3017.
17) E. Sato, K. Sato and Y. Tamakawa: Annu. Rep. Iwate Med. Univ. School Lib. Arts Sci. **35** (2000) 13.
18) B. K. Agarwal: *X-ray Spectroscopy* (Springer-Verlag, New York, 1991) 2nd ed., p. 18.

Japanese Journal of Applied Physics
Vol. 44, No. 12, 2005, pp. 8716–8721



# Enhanced K-edge Angiography Utilizing Tantalum Plasma X-ray Generator in Conjunction with Gadolinium-Based Contrast Media

Eiichi SATO, Yasuomi HAYASI, Koji KIMURA[1], Etsuro TANAKA[2], Hidezo MORI[3], Toshiaki KAWAI[4], Takashi INOUE[5], Akira OGAWA[5], Shigehiro SATO[6], Kazuyoshi TAKAYAMA[7], Jun ONAGAWA[8] and Hideaki IDO[8]

*Department of Physics, Iwate Medical University, 3-16-1 Honchodori, Morioka 020-0015, Japan*
[1]*Department of Physiology, Tokai University School of Medicine, Boseidai, Isehara, Kanagawa 259-1193, Japan*
[2]*Department of Nutritional Science, Faculty of Applied Bio-science, Tokyo University of Agriculture, 1-1-1 Sakuragaoka, Setagaya-ku, Tokyo 156-8502, Japan*
[3]*Department of Cardiac Physiology, National Cardiovascular Center Research Institute, 5-7-1 Fujishirodai, Suita, Osaka 565-8565, Japan*
[4]*Electron Tube Division #2, Hamamatsu Photonics K.K., 314-5 Shimokanzo, Toyooka Village, Iwata, Shizuoka 438-0193, Japan*
[5]*Department of Neurosurgery, School of Medicine, Iwate Medical University, 19-1 Uchimaru, Morioka 020-8505, Japan*
[6]*Department of Microbiology, School of Medicine, Iwate Medical University, 19-1 Uchimaru, Morioka 020-8505, Japan*
[7]*Shock Wave Research Center, Institute of Fluid Science, Tohoku University, 2-1-1 Katahira, Sendai 980-8577, Japan*
[8]*Department of Applied Physics and Informatics, Faculty of Engineering, Tohoku Gakuin University, 1-13-1 Chuo, Tagajo, Miyagi 985-8537, Japan*

(Received June 5, 2005; accepted August 17, 2005; published December 8, 2005)

The tantalum plasma flash X-ray generator is useful for performing high-speed enhanced K-edge angiography using cone beams because K-series characteristic X-rays from the tantalum target are absorbed effectively by gadolinium-based contrast media. In the flash X-ray generator, a 150 nF condenser is charged up to 80 kV by a power supply, and flash X-rays are produced by the discharging. The X-ray tube is a demountable cold-cathode diode, and the turbomolecular pump evacuates air from the tube with a pressure of approximately 1 mPa. Since the electric circuit of the high-voltage pulse generator employs a cable transmission line, the high-voltage pulse generator produces twice the potential of the condenser charging voltage. At a charging voltage of 80 kV, the estimated maximum tube voltage and current were approximately 160 kV and 40 kA, respectively. When the charging voltage was increased, the K-series characteristic X-ray intensities of cerium increased. The K lines were clean and intense, and hardly any bremsstrahlung rays were detected. The X-ray pulse widths were approximately 100 ns, and the time-integrated X-ray intensity had a value of approximately 300 μGy at 1.0 m from the X-ray source with a charging voltage of 80 kV. Angiography was performed using a filmless computed radiography (CR) system and gadolinium-based contrast media. In the angiography of nonliving animals, we observed fine blood vessels of approximately 100 μm with high contrasts. [DOI: 10.1143/JJAP.44.8716]

KEYWORDS: angiography, gadolinium-based contrast media, characteristic X-rays, quasi-monochromatic X-rays, tantalum K lines

## 1. Introduction

Enhanced K-edge angiography[1–4] has been performed utilizing monochromatic parallel X-ray beams produced from synchrotron orbital radiation using a monochrocollimator. The photon energies of the beams are approximately 35 keV, and are absorbed effectively by iodine-based contrast media with a K-absorption edge of 33.2 keV. Nowadays, an X-ray generator with a cerium-target tube[5] can be used in order to perform the K-edge angiography because K-series characteristic X-rays with photon energies just beyond the K-edge are absorbed effectively by iodine.

To perform high-speed biomedical radiography, we have developed several different high-dose-rate X-ray generators corresponding to specific objectives. For example, flash X-ray generators[6–9] with cold-cathode tubes produce extremely short X-ray pulses with durations of less than 1 μs, and the X-ray duration can be controlled accurately from 10 μs to 1.0 ms in cases where stroboscopic X-ray generators[10,11] utilizing hot-cathode triodes are employed.

Recently, although clean K-series characteristic X-rays of copper[12] and nickel[13] have been produced using plasma flash X-ray generators, low-intensity bremsstrahlung X-rays have been observed using a molybdenum target.[14] Therefore, we have performed preliminary experiments for producing clean high-photon-energy characteristic X-rays from molybdenum, silver and cerium targets using a compact flash X-ray generator with a disk-cathode tube,[15] and have succeeded in producing clean characteristic X-rays using the angle dependence of bremsstrahlung X-ray distributions. However, the X-ray intensity should be increased to a sufficient level for iodine angiography by increasing the electrostatic energies in the generator.

Since K-series characteristic X-rays from ytterbium, tantalum, and tungsten targets are absorbed effectively by gadolinium-based contrast media used in MRA, these X-rays are very useful for performing enhanced K-edge angiography. As compared with K-edge angiography using an iodine medium with an X-ray photon energy of 35 keV, the absorbed dose can be decreased easily in cases where the gadolinium medium is employed.

In the present research, we developed an intense quasi-monochromatic plasma flash X-ray generator with a tantalum target tube, and used it to perform a preliminary study on angiography achieved with tantalum K-series characteristic X-rays.

## 2. Principle of Angiography

Figure 1 shows the mass attenuation coefficients of gadolinium at the selected energies; the coefficient curve is discontinuous at the gadolinium K-edge. The average photon energy of the tantalum Kα lines is shown above the gadolinium K-edge. The average photon energy of tantalum Kα lines is 57.1 keV, and gadolinium contrast media with a K-absorption edge of 50.2 keV absorb the lines easily. Therefore, blood vessels were observed with high contrasts.

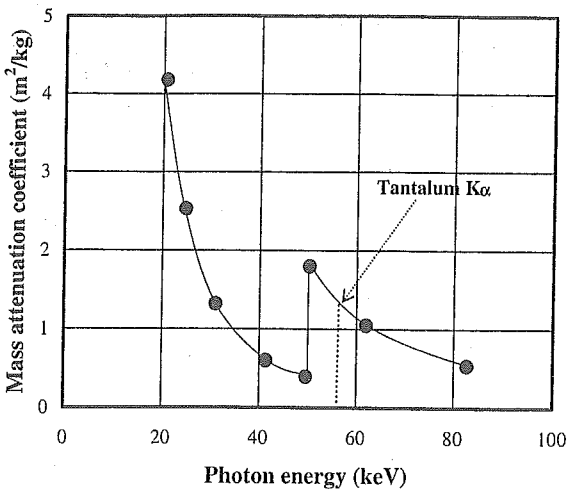


Fig. 1. Mass attenuation coefficient of gadolinium. The average photon energy of tantalum Kα lines is shown above the gadolinium K-edge.

## 3. Generator

### 3.1 *High-voltage circuit*

Figure 2 shows a block diagram including the electric circuit of a high-intensity plasma flash X-ray generator. The generator consists of the following essential components: a high-voltage power supply, a high-voltage condenser with a capacity of approximately 150 nF, an air gap switch, a turbomolecular pump, a thyratron pulse generator as a trigger device, and a flash X-ray tube. In this generator, a coaxial cable transmission line is employed in order to increase maximum tube voltage using high-voltage reflection. The high-voltage main condenser is charged up to 80 kV by the power supply, and electric charges in the condenser are discharged to the tube through the four cables after closing the gap switch with the trigger device.

### 3.2 *X-ray tube*

The X-ray tube is a demountable cold-cathode diode that is connected to the turbomolecular pump with a pressure of approximately 1 mPa (Fig. 3). This tube consists of the following major parts: a ring-shaped graphite cathode with an inside diameter of 4.5 mm, a stainless-steel vacuum chamber, a nylon insulator, a polyethylene terephthalate (Mylar) X-ray window 0.25 mm in thickness, and a rod-shaped tantalum target 3.0 mm in diameter. The distance between the target and cathode electrodes can be regulated from the outside of the tube, and is set to 1.5 mm. As electron beams from the cathode electrode are roughly converged to the target by the electric field in the tube, evaporation leads to the formation of weakly ionized plasma, consisting of tantalum ions and electrons, around the target. Because bremsstrahlung rays are not emitted in the opposite direction to that of the electron trajectory in Sommerfeld's theory[16] (Fig. 4), tantalum K-series characteristic X-rays can be produced without using a filter.

## 4. Characteristics

### 4.1 *Tube voltage and current*

In this generator, it was difficult to measure the tube voltage and current since the tube voltages were high, and there was no space to set a current transformer for measuring the tube current. Currently, the voltage and current roughly display damped oscillations. When the charging voltage was increased, both the maximum tube voltage and current increased. At a charging voltage of 80 kV, the estimated maximum values of the tube voltage and current were approximately 160 kV (two times the charging voltage) and 40 kA, respectively.

### 4.2 *X-ray output*

The X-ray output pulse was detected using a combination of a plastic scintillator and a photomultiplier (Fig. 5). The X-ray pulse height substantially increased with charging

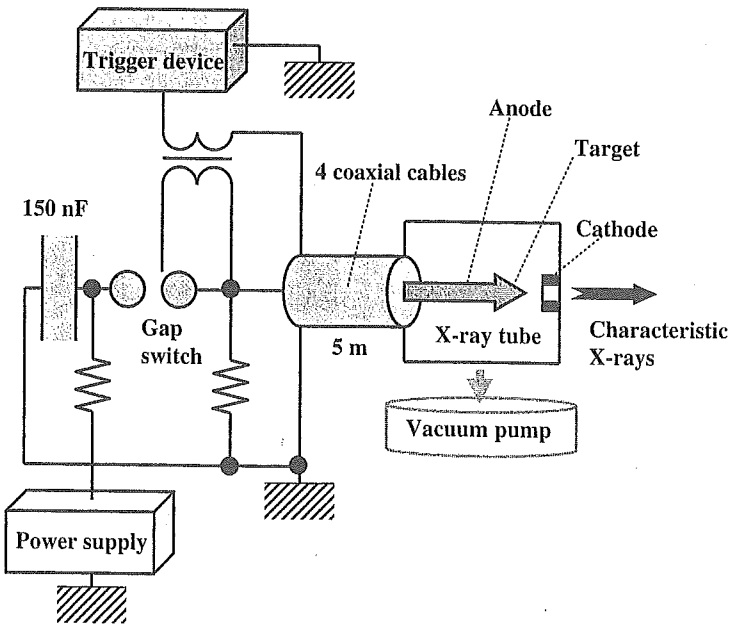


Fig. 2. Block diagram including high-voltage circuit of intense quasi-monochromatic plasma flash X-ray generator with tantalum-target tube.

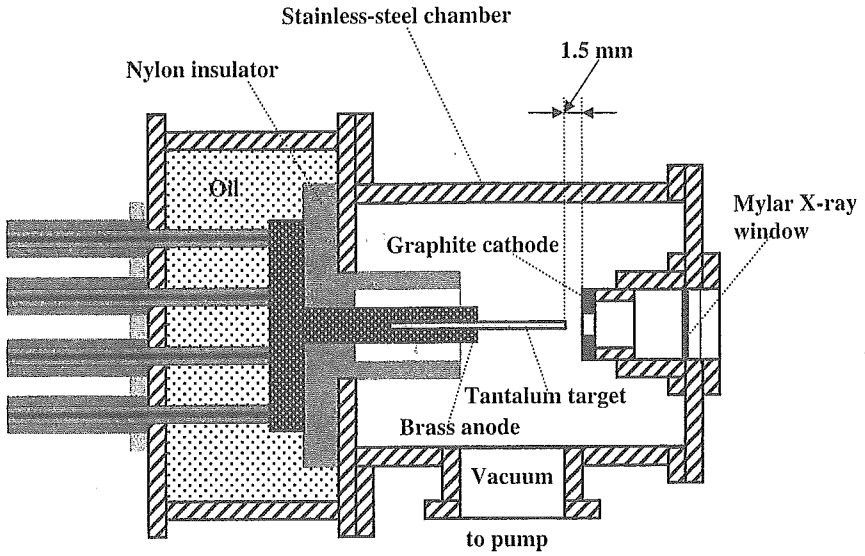


Fig. 3. Schematic drawing of flash X-ray tube with rod-shaped tantalum target.

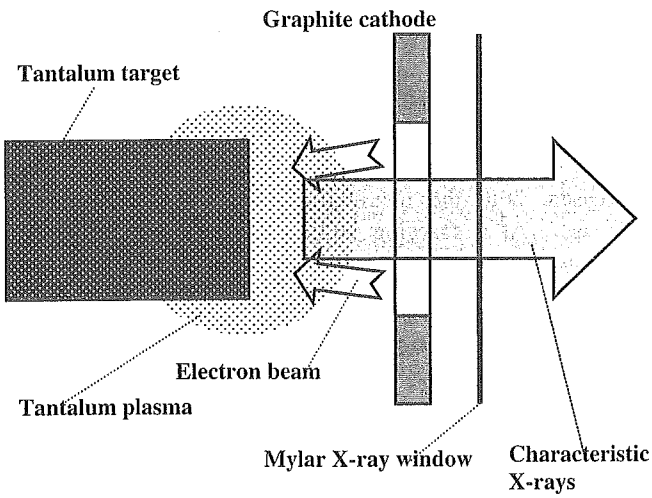


Fig. 4. Irradiation of K-series characteristic X-rays of tantalum.

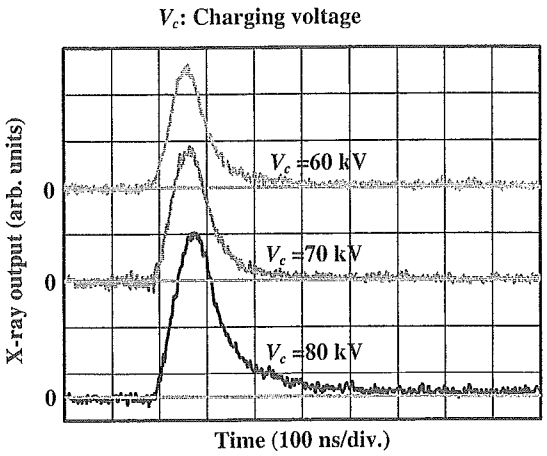


Fig. 5. X-ray outputs detected using combination of plastic scintillator and photomultiplier.

voltage. The X-ray pulse widths were approximately 100 ns, and the time-integrated X-ray intensity measured by a thermoluminescence dosimeter (Kyokko TLD Reader 1500 having MSO-S elements without energy compensation) had a value of approximately 300 μGy per pulse at 1.0 m from the X-ray source with a charging voltage of 80 kV.

### *4.3 X-ray source*

In order to observe the characteristic X-ray source, we employed a 100-μm-diameter pinhole camera and an X-ray film (Polaroid XR-7) (Fig. 6). When the charging voltage was increased, the plasma X-ray source grew, and both spot dimension and intensity increased. Because the X-ray intensity is the highest at the center of the spot, both the dimension and intensity decreased as the thickness of a filter for absorbing X-rays increased and as the pinhole diameter decreased.

### *4.4 X-ray spectra*

X-ray spectra were measured using a transmission-type spectrometer[14] with a lithium fluoride curved crystal 0.5 mm

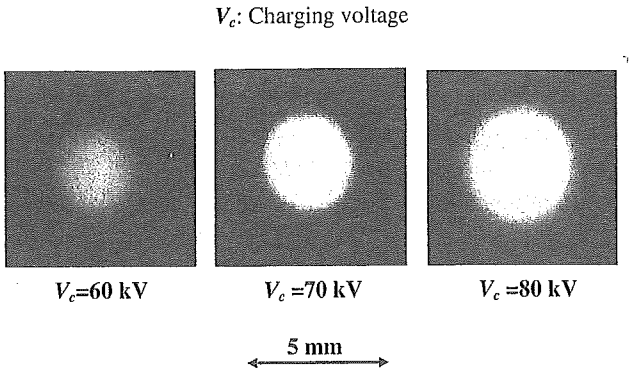


Fig. 6. Images of characteristic X-ray source obtained using pinhole camera with changes in charging voltage.

in thickness. The X-ray intensities of the spectra were detected by an imaging plate of a CR system[17] (Konica Regius 150) with a wide dynamic range, and relative X-ray intensity was calculated from Dicom original digital data corresponding to X-ray intensity; the data was scanned by a

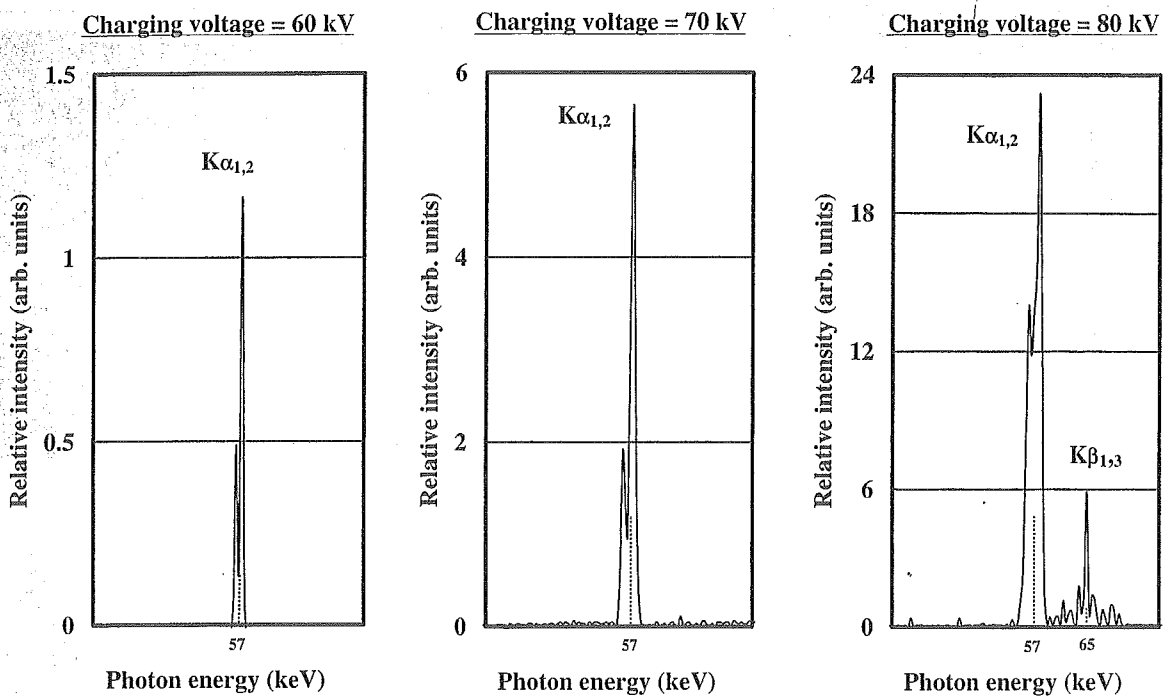


Fig. 7. X-ray spectra from tantalum target. Spectra were measured using a transmission-type spectrometer with a lithium fluoride curved crystal.

Dicom viewer in the filmless CR system. Subsequently, the relative X-ray intensity as a function of the data was calibrated using a conventional X-ray generator, and we confirmed that the intensity was proportional to the exposure time. Figure 7 shows measured spectra from the tantalum target. We observed clean K-series lines, while bremsstrahlung rays were hardly detected. The characteristic X-ray intensity substantially increased with charging voltage.

## 5. Angiography

Flash angiography was performed using the CR system at 1.2 m from the X-ray source, and the charging voltage was 80 kV. First, rough measurements of spatial resolution were made using wires. Figure 8 shows radiograms of tungsten wires in a rod made of poly(methyl methacrylate) (PMMA). Although the image contrast decreased slightly with wire diameter, due to blurring of the image caused by the sampling pitch of 87.5 μm, a 50-μm-diameter wire could be observed. Because the tungsten wires transmitted the characteristic X-rays easily, low-contrast radiograms were obtained.

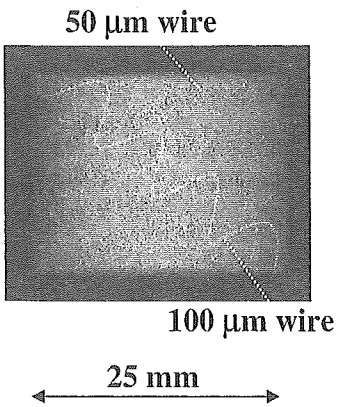


Fig. 8. Radiograms of tungsten wires in PMMA rod.

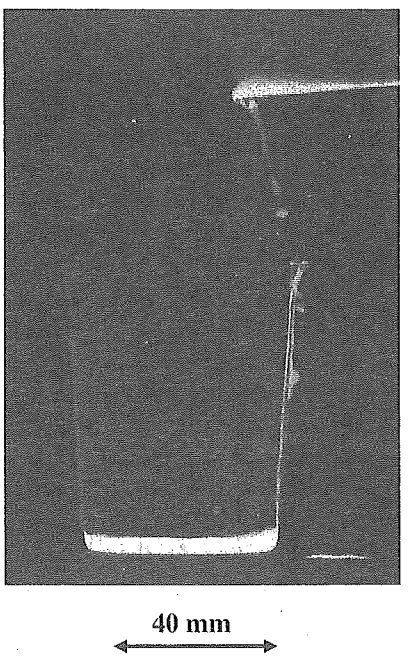


Fig. 9. Radiogram of water (20% gadolinium oxide suspension) falling into polypropylene beaker from glass test tube.

The image of water (gadolinium oxide suspension of 20%) falling into a polypropylene beaker from a plastic test tube is shown in Fig. 9. The diameter of gadolinium oxide powder ranges from 1 to 10 μm. Because the X-ray duration was about 100 ns, the stop-motion image of water could be obtained.

Figure 10 shows an angiogram of poly(tetrafluoroethylene) (Teflon) tubes of 0.5 and 1.0 mm bore diameter in a

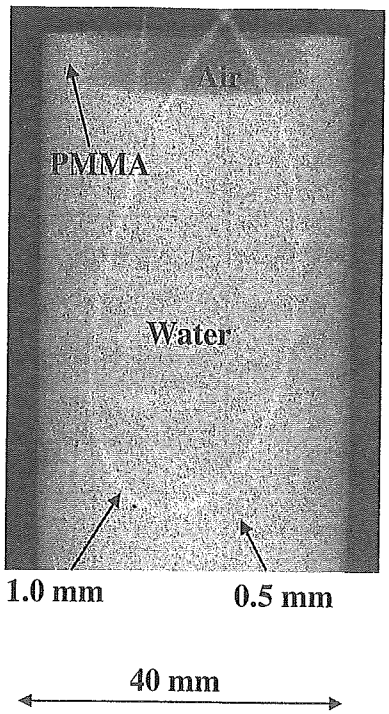


Fig. 10. Angiography of Teflon tube using contrast medium which contains approximately 65% gadodiamidehydrate.

PMMA case using a contrast medium which contains approximately 65% gadodiamidehydrate; the 0.5 mm tube can be observed easily. Figure 11 shows an angiogram of a rabbit head using gadolinium oxide powder, and fine blood vessels of approximately 100 μm were visible.

## 6. Discussion

In summary, we succeeded in producing K-series characteristic X-rays of tantalum and in performing K-edge angiography using gadolinium contrast media with a K-edge of 50.2 keV; this K-edge angiography could be a useful technique for reducing the dose absorbed by patients. Although we employed tantalum K$\alpha$ (57.1 keV) and K$\beta$ (approximately 65 keV) rays, K$\beta$ rays should be absorbed using an ytterbium oxide filter in order to increase the image contrast of blood vessels. In addition, L-series characteristic rays should be absorbed before angiography using a tungsten or an ytterbium oxide filter. In these cases, the photon energies of the K-absorption edges of tungsten and ytterbium are 69.5 and 61.3 keV, respectively.

In cases where a high tube voltage beyond the critical excitation potential is applied, the optimum intensity for angiography can be controlled because the K-series characteristic intensity substantially increases with charging voltage. In this research, the generator-produced instantaneous number of K photons was approximately $1 \times 10^9$ photons/cm$^2$ per pulse at 1.0 m from the source.

Using this flash X-ray generator, because the photon energy of characteristic X-rays can be selected, quasi-monochromatic imaging, such as enhanced K-edge angiography using iodine contrast media and mammography, can be performed. In addition, steady-state monochromatic X-rays can be produced by a similar tube utilizing a hot cathode and a constant high-voltage power supply. In conjunction with the fine focusing technique, these monochromatic X-ray generators could be employed to perform K-edge angiography and X-ray phase-contrast radiography for edge enhancement.

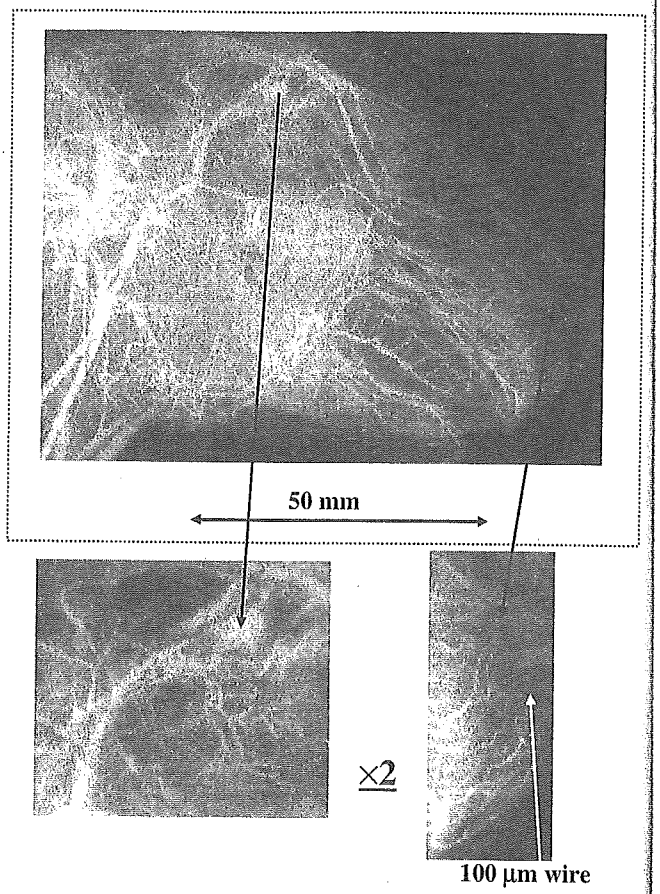


Fig. 11. Angiography of rabbit head using gadolinium oxide powder.

## Acknowledgment

This work was supported by Grants-in-Aid for Scientific Research (13470154, 13877114, 16591181, and 16591222) and Advanced Medical Scientific Research from MECSST, Health and Labor Sciences Research Grants (RAMT-nano-001, RHGTEFB-genome-005 and RHGTEFB-saisei-003), Grants from the Keiryo Research Foundation, The Promotion and Mutual Aid Corporation for Private Schools of Japan, the Japan Science and Technology Agency (JST), and the New Energy and Industrial Technology Development Organization (NEDO, Industrial Technology Research Grant Program in '03).

1) A. Akisada, M. Ando, K. Hyodo, S. Hasegawa, K. Konishi, K. Nishimura, A. Maruhashi, F. Toyofuku, A. Suwa and K. Kohra: Nucl. Instrum. Methods Phys. Res., Sect. A **246** (1986) 713.
2) A. C. Thompson, H. D. Zeman, G. S. Brown, J. Morrison, P. Reiser, V. Padmanabahn, L. Ong, S. Green, J. Giacomini, H. Gordon and E. Rubenstein: Rev. Sci. Instrum. **63** (1992) 625.
3) H. Mori *et al.*: Radiology **201** (1996) 173.
4) K. Hyodo, M. Ando, Y. Oku, S. Yamamoto, T. Takeda, Y. Itai, S. Ohtsuka, Y. Sugishita and J. Tada: J. Synchrotron Radiat. **5** (1998) 1123.
5) E. Sato, E. Tanaka, H. Mori, T. Kawai, T. Ichimaru, S. Sato, K. Takayama and H. Ido: Med. Phys. **31** (2004) 3017.
6) E. Sato, S. Kimura, S. Kawasaki, H. Isobe, K. Takahashi, Y. Tamakawa and T. Yanagisawa: Rev. Sci. Instrum. **61** (1990) 2343.
7) A. Shikoda, E. Sato, M. Sagae, T. Oizumi, Y. Tamakawa and T.

Yanagisawa: Rev. Sci. Instrum. **65** (1994) 850.
8) K. Takahashi, E. Sato, M. Sagae, T. Oizumi, Y. Tamakawa and T. Yanagisawa: Jpn. J. Appl. Phys. **33** (1994) 4146.
9) E. Sato, K. Takahashi, M. Sagae, S. Kimura, T. Oizumi, Y. Hayasi, Y. Tamakawa and T. Yanagisawa: Med. Biol. Eng. Comput. **32** (1994) 289.
10) E. Sato, M. Sagae, K. Takahashi, A. Shikoda, T. Oizumi, Y. Hayasi, Y. Tamakawa and T. Yanagisawa: Med. Biol. Eng. Comput. **32** (1994) 295.
11) E. Sato, Y. Hayasi and Y. Tamakawa: Annu. Rep. Iwate Med. Univ. Lib. Arts Sci. **35** (2000) 1.
12) E. Sato, Y. Hayasi, R. Germer, E. Tanaka, H. Mori, T. Kwai, T. Ichimaru, K. Takayama and H. Ido: Rev. Sci. Instrum. **74** (2003) 5236.
13) E. Sato, Y. Hayasi, R. Germer, E. Tanaka, H. Mori, T. Kawai, T. Ichimaru, S. Sato, K. Takayama and H. Ido: J. Electron Spectrosc. Relat. Phenom. C **137–140** (2004) 713.
14) E. Sato, Y. Hayasi, R. Germer, E. Tanaka, H. Mori, T. Kawai, H. Obara, T. Ichimaru, K. Takayama and H. Ido: Jpn. J. Med. Phys. **20** (2003) 123.
15) E. Sato, E. Tanaka, H. Mori, T. Kawai, T. Ichimaru, S. Sato, K. Takayama and H. Ido: Med. Phys. **32** (2005) 49.
16) B. K. Agarwal: *X-ray Spectroscopy* (Springer-Verlag, New York, 1991) 2nd ed., p. 18.
17) E. Sato, K. Sato and Y. Tamakawa: Annu. Rep. Iwate Med. Univ. Sch. Lib. Arts Sci. **35** (2000) 13.

# Enhanced magnification angiography including phase-contrast effect using a 100-μm focus x-ray tube

Eiichi Sato*[a], Etsuro Tanaka[b], Hidezo Mori[c], Hiroki Kawakami[d], Toshiaki Kawai[d], Takashi Inoue[e], Akira Ogawa[e], Shigehiro Sato[f], Toshio Ichimaru[g], Kazuyoshi Takayama[h] and Hideaki Ido[i]

[a] Department of Physics, Iwate Medical University, 3-16-1 Honchodori, Morioka 020-0015, Japan
[b] Department of Nutritional Science, Faculty of Applied Bio-science, Tokyo University of Agriculture, 1-1-1 Sakuragaoka, Setagaya-ku 156-8502, Japan
[c] Department of Cardiac Physiology, National Cardiovascular Center Research Institute, 5-7-1 Fujishirodai, Suita, Osaka 565-8565 Japan
[d] Electron Tube Division #2, Hamamatsu Photonics K. K., 314-5 Shimokanzo, Iwata 438-0193, Japan
[e] Department of Neurosurgery, School of Medicine, Iwate Medical University, 19-1 Uchimaru, Morioka 020-8505, Japan,
[f] Department of Microbiology, School of Medicine, Iwate Medical University, 19-1 Uchimaru, Morioka 020-8505, Japan
[g] Department of Radiological Technology, School of Health Sciences, Hirosaki University, 66-1 Honcho, Hirosaki 036-8564, Japan
[h] Shock Wave Research Center, Institute of Fluid Science, Tohoku University, 2-1-1 Katahira, Sendai 980-8577, Japan
[i] Department of Applied Physics and Informatics, Faculty of Engineering, Tohoku Gakuin University, 1-13-1 Chuo, Tagajo 985-8537, Japan

## ABSTRACT

A microfocus x-ray tube is useful in order to perform magnification digital radiography including phase-contrast effect. The 100-μm-focus x-ray generator consists of a main controller for regulating the tube voltage and current and a tube unit with a high-voltage circuit and a fixed anode x-ray tube. The maximum tube voltage, current, and electric power were 105 kV, 0.5 mA, and 50 W, respectively. Using a 3-mm-thick aluminum filter, the x-ray intensity was 26.0 μGy/s at 1.0 m from the source with a tube voltage of 60 kV and a current of 0.50 mA. Because the peak photon energy was approximately 38 keV using the filter with a tube voltage of 60 kV, the bremsstrahlung x-rays were absorbed effectively by iodine-based contrast media with an iodine K-edge of 33.2 keV. Magnification angiography including phase-contrast effect was performed by three-time magnification imaging with a computed radiography system using iodine-based microspheres 15 μm in diameter. In angiography of non-living animals, we observed fine blood vessels of approximately 100 μm with high contrasts.

**Keywords:** high-contrast angiography, magnification digital radiography, microfocus x-ray tube, energy-selective imaging, phase-contrast effect

## 1. INTRODUCTION

Conventional flash x-ray generators utilizing condensers are useful in order to perform high-speed radiography including biomedical applications, and several different generators have been developed.[1-7] In particular, plasma flash x-ray generators[8-10] have been employed to produce clean K-series characteristic x-rays, and we have confirmed the irradiation of higher harmonic hard x-rays of Kα and Kβ lines. Without forming plasmas, demountable flash x-ray tubes can be employed to perform fundamental study on producing monochromatic x-rays,[11,12] and have succeeded in producing clean characteristic x-rays using angle dependence of bremsstrahlung x-ray distribution in Sommerfeld's theory. However, monochromatic flash radiography has had difficulties in increasing x-ray duration, and in performing magnification

Laser-Generated, Synchrotron, and Other Laboratory X-Ray and EUV Sources, Optics, and Applications II Edited by Kyrala, Gauthier, MacDonald, Khounsary
Proc. of SPIE Vol. 5918, 591811, (2005) · 0277-786X/05/$15 · doi: 10.1117/12.620205

radiography including phase-contrast effect.
Synchrotrons are capable of producing high-dose-rate monochromatic parallel x-ray beams using a monochrocollimator, and the beams have been applied to phase-contrast radiography[13,14] and enhanced K-edge angiography.[15,16] In angiography, monochromatic x-rays with photon energies approximately 35 keV have been employed because the rays are absorbed effectively by iodine-based contrast media with an iodine K edge of 33.2 keV.
Without using synchrotrons, phase-contrast radiography for edge enhancement can be performed using a microfocus x-ray tube, and the enhancement have been applied in mammography achieved with a computed radiography (CR) system[17] using a 100-μm-focus molybdenum tube.[18] Subsequently, we have developed a cerium x-ray generator[19,20] to perform enhanced K-edge angiography using cone beams, and have succeeded in observing fine blood vessels and coronary arteries with high contrasts using cerium Kα rays of 34.6 keV. However, it is difficult to design the small focus cerium tube for angiography.
The magnification radiography is useful in order to improve the spatial resolution in digital radiography, and the phase contrast may come into effect in edge enhancement of comparatively large objects including thick blood vessels filled with low-density contrast media. Therefore, narrow photon energy bremsstrahlung x-rays with a peak energy of approximately 35 keV from a microfocus tungsten tube are useful to perform high-contrast high-resolution angiography. In the present research, we employed a 100-μm-focus tungsten tube, and performed enhanced magnification angiography including phase-contrast effect by controlling bremsstrahlung x-ray spectra using an aluminum filter.

## 2. PRINCIPLE OF ENHANCED ANGIOGRAPHY

Figure 1 shows the mass attenuation coefficients of iodine at the selected energies; the coefficient curve is discontinuous at the iodine K-edge. The effective bremsstrahlung x-ray spectra for K-edge angiography are shown above the iodine K-edge. Because iodine contrast media with a K-absorption edge of 33.2 keV absorb the rays easily, blood vessels were observed with high contrasts.

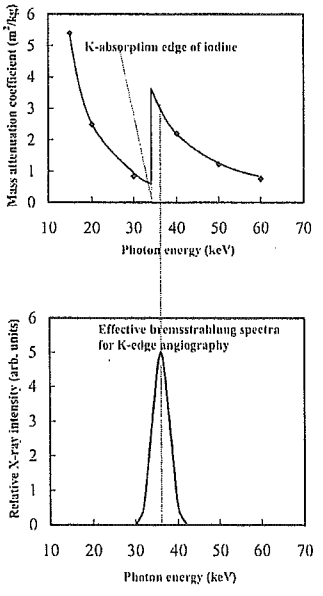


Figure 1: Mass attenuation coefficients of iodine and effective bremsstrahlung x-rays for enhanced K-edge angiography.

## 3. EXPERIMENTAL SETUP

Figure 2 shows the block diagram of a microfocus x-ray generator used in this experiment, and the generator consists of a main controller, an x-ray tube unit with a Cockcroft-Walton circuit, an insulation transfprmer, and a 100-μm-focus x-ray tube. The tube voltage, the current, and the exposure time can be controlled by the controlle. The main circuit for producing x-rays is illustrated in Fig. 3, and employed the Cockcroft-Walton circuit in order to decrease the dimensions of the tube unit. In the x-ray tube, the positive and negative high voltages are applied to the anode and cathode electrodes,

respectively. The filament heating current is supplied by an AC power supply in the controller in conjunction with an insulation transformer which is used for isolation from the high voltage from the Cockcroft-Walton circuit. In this experiment, the tube voltage applied was from 45 to 70 kV, and the tube current was regulated to within 0.50 mA (maximum current) by the filament temperature. The exposure time is controlled in order to obtain optimum x-ray intensity, and narrow-photon-energy bremsstrahlung x-rays are produced using a 3.0-mm-thick aluminum filter for absorbing soft x-rays.

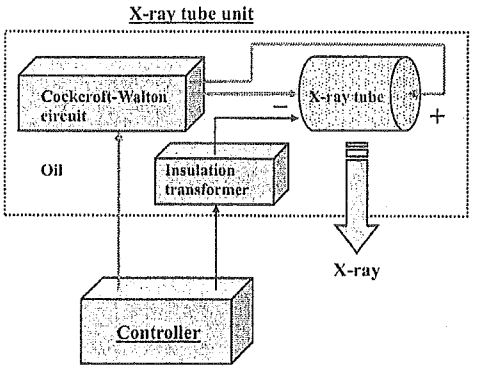


Figure 2: Block diagram of the x-ray generator.

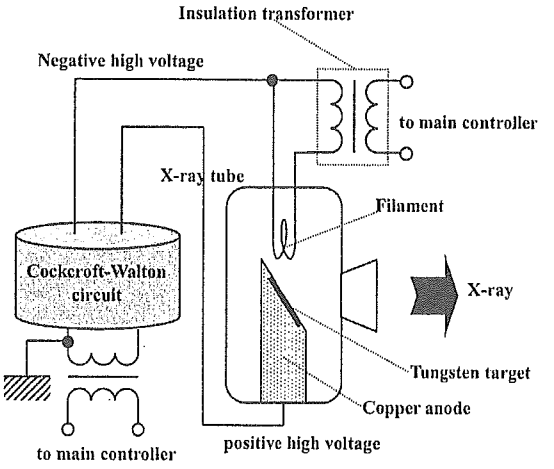


Figure 3: Electric circuit of the x-ray generator.

## 4 RESULTS

### 4.1 *X-ray intensity*

The x-ray intensity was measured by a Victoreen 660 ionization chamber at 1.0 m from the x-ray source using the filter (Fig. 4). At a constant tube current of 0.50 mA, the x-ray intensity increased when the tube voltage was increased. At a tube voltage of 60 kV, the intensity with the filter was 26.0 μGy/s.

### 4.2 *X-ray spectra*

In order to measure x-ray spectra, we employed a cadmium telluride detector (CDTE2020X, Hamamatsu Photonics K. K.) with a photon energy resolution of approximately 1.7 keV (Fig. 5). When the tube voltage was increased, the bremsstrahlung x-ray intensity increased, and both the maximum photon energy and the spectrum peak energy increased.

In order to perform K-edge angiography, bremsstrahlung x-rays of approximately 35 keV are useful, and the high-energy bremsstrahlung x-rays decrease the image contrast. Using this filter, because bremsstrahlung x-rays with energies higher than 60 keV were not absorbed easily, the tube voltage for angiography was determined as 60 kV.

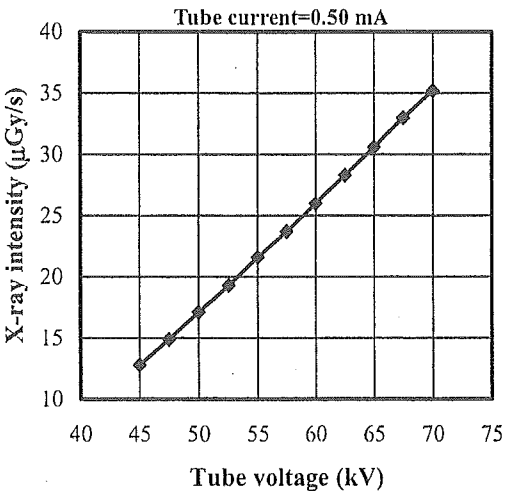


Figure 4: X-ray intensity (μGy/s) as a function of tube voltage (kV) with a tube current of 0.50 mA.

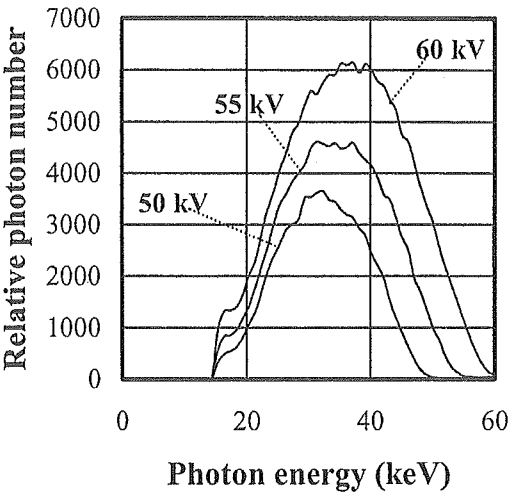


Figure 5. Bremsstrahlung x-ray spectra measured using a cadmium telluride detector with changes in the tube voltage.

### 4.3 *Magnification radiography*

The magnification radiography was performed by three-time magnification imaging using the CR system and the filter at a tube voltage of 60 kV, and the distance (between the x-ray source and the imaging plate) was 1.5 m (Fig. 6). Firstly, the spatial resolutions of conventional (cohesion) and magnification radiographies were made using a lead test chart. In the magnification radiography, 50 μm lines (10 line pairs) were clearly visible (Fig. 7). Subsequently, Fig. 8 shows radiograms of tungsten wires coiled around rods made of polymethyl methacrylate (PMMA). Although the image contrast decreased somewhat with decreases in the wire diameter, due to blurring of the image caused by the sampling pitch of 87.5 μm, a 50-μm-diameter wire could be observed. Radiograms of one set of a bolt and a nut are shown in Fig. 9, the edge of a bubble in the bolt and the seam between the bolt and the nut are visible in magnification radiography.

### 4.4 *Enhanced magnification angiography*

The magnification angiography was performed at the same conditions using iodine microspheres of 15 μm in diameter, and the microspheres (containing 37% iodine by weight) are very useful for making phantoms of non-living animals used for angiography. Angiogram of a rabbit heart is shown in Fig. 10, and the coronary arteries are visible. Figure 11 shows angiograms of a larger dog heart using iodine spheres. Although the image contrast decreased slightly with increases in the thickness of the PMMA plate facing the x-ray source, the coronary arteries of approximately 100 μm were observed using a 100-mm-thick plate.

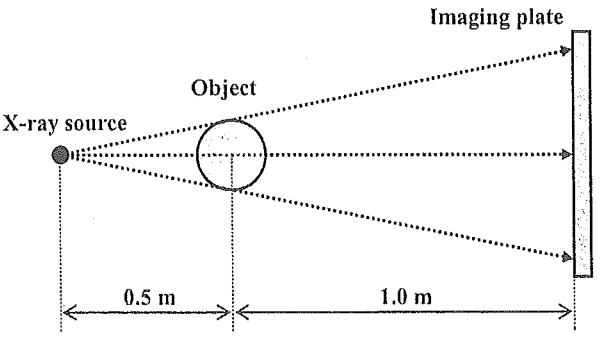


Figure 6. Three-time magnification imaging using an imaging plate in conjunction with a microfocus tube.

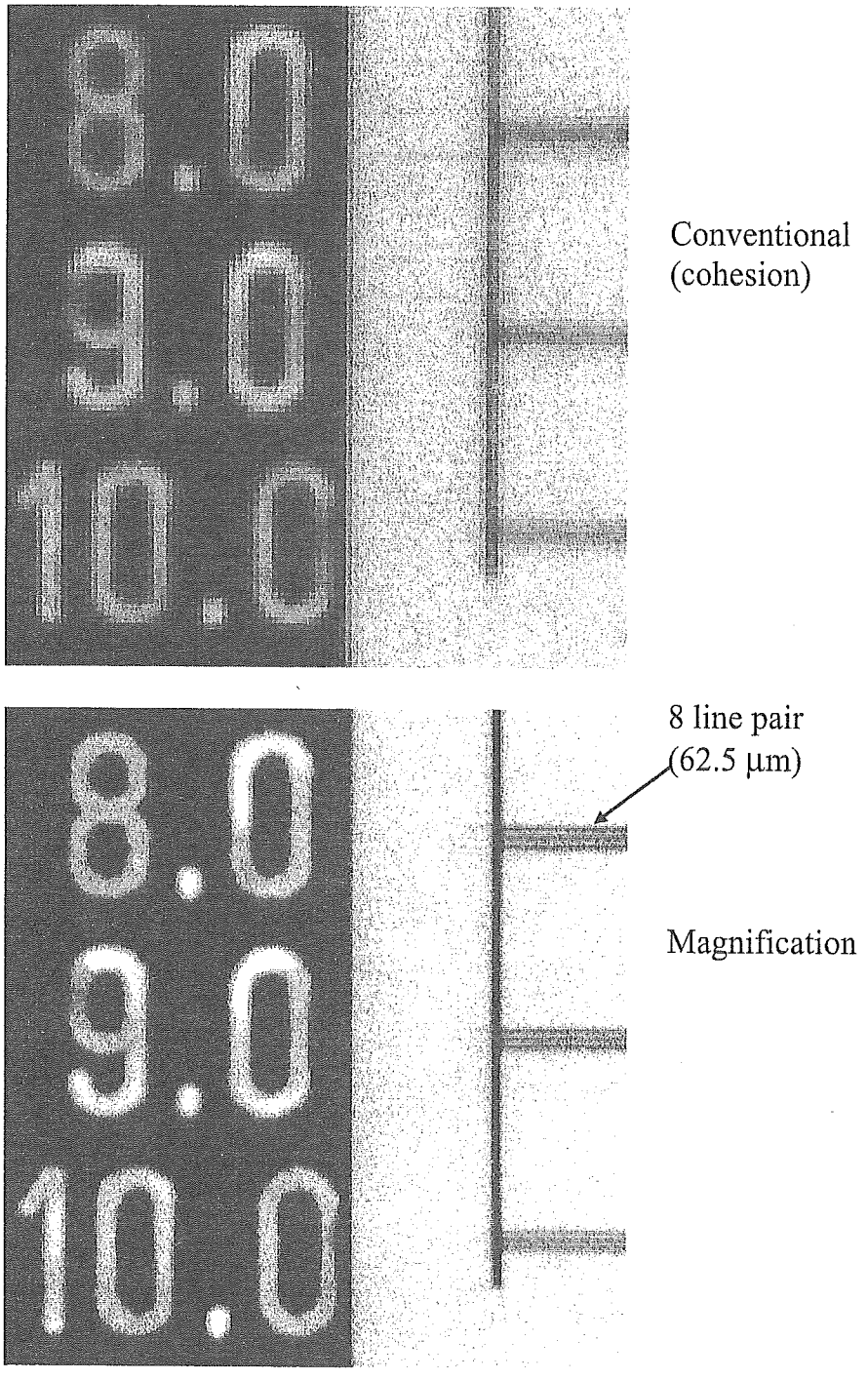


Figure 7. Radiogram of a test chart for measuring the spatial resolution.

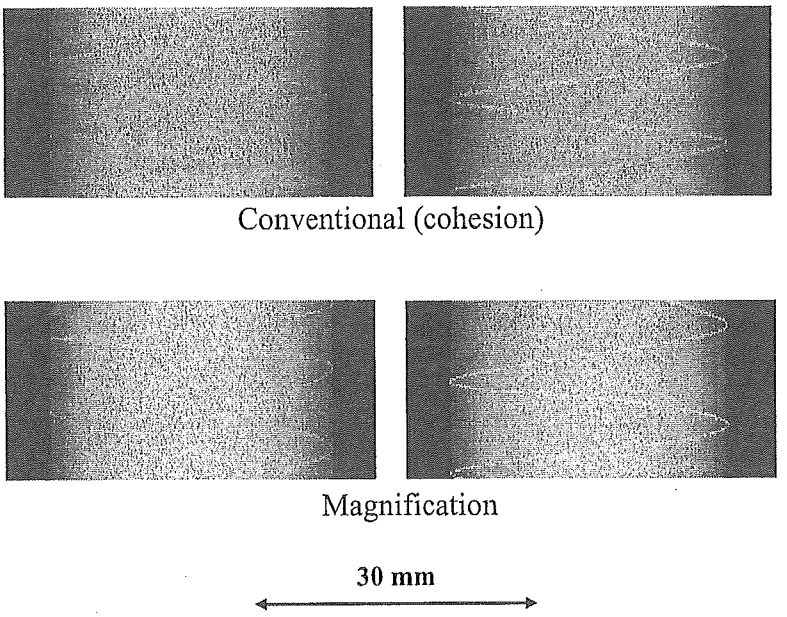


Figure 8. Radiograms of tungsten wires coiled around PMMA rods.

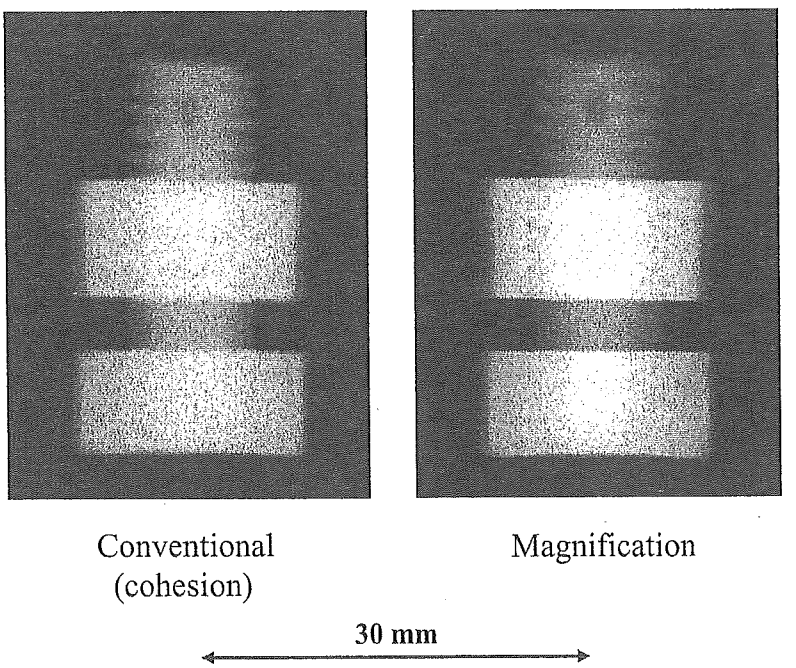


Figure 9. Radiograms of a set of a plastic bolt and a nut.

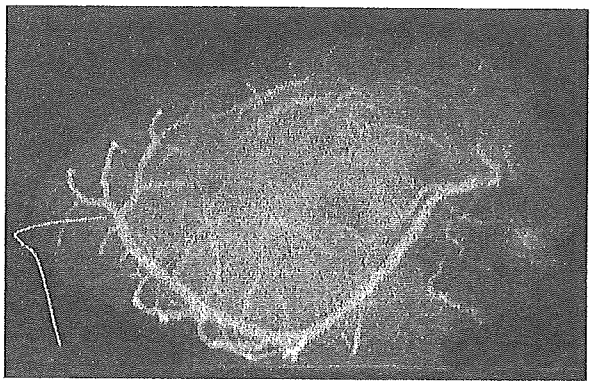

Figure 10: Angiogram of an extracted rabbit heart using iodine microspheres.

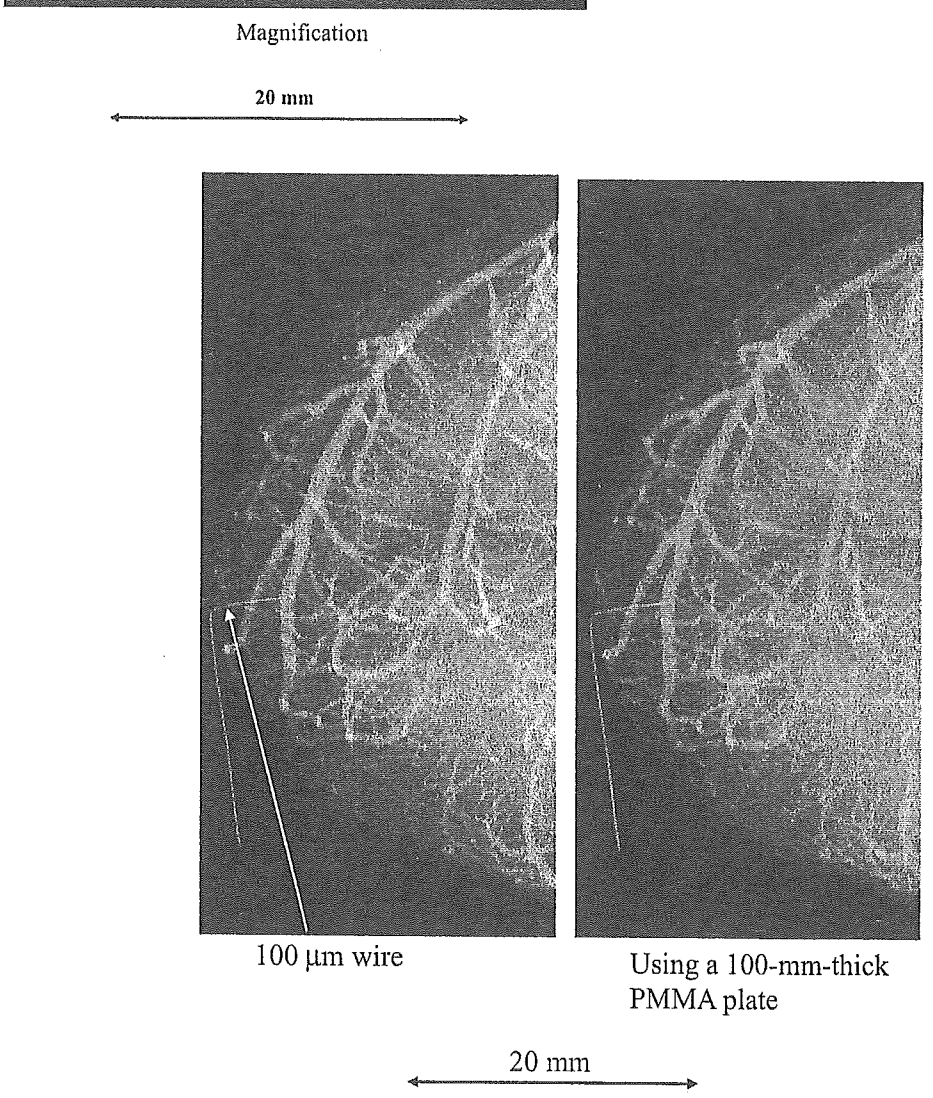


Figure 11. Angiograms of an extracted dog heart.

## 5. CONCLUSIONS AND OUTLOOK

In summary, we employed an x-ray generator with a 100-μm-focus tungsten tube and performed enhanced magnification angiography including phase-contrast effect using narrow-photon-energy bremsstrahlung x-rays with a peak photon energy of approximately 38 keV, which can be absorbed easily by iodine-based contrast media. The bremsstrahlung x-ray intensity substantially increased with increases in the tube voltage, and the tube voltage was determined as 60 kV in order to increase the image contrast. In enhanced angiography, although we obtained almost absorption-contrast images, phase-contrast effect may be added in cases where low-density media are employed.

Because the sampling pitch of the CR system is 87.5 μm, we obtained spatial resolutions of approximately 50 μm using 3-time magnification imaging even when a 100-μm-focus tube was employed. In order to observe fine blood vessels of less than 100 μm, the spatial resolution of the CR system should be improved to 43.8 μm (Konica Minolta Regius 190), and the iodine density should be increased.

At a tube voltage of 60 kV and a current of 0.50 mA, the maximum number of photons was approximately $4\times10^7$ photons/cm$^2$·s at 1.0 m from the source, and the photon count rate can be increased easily using a rotating anode microfocus tube developed by Hitachi Medical Corporation. Recently, the maximum electric power of the microfocus x-ray tube has been increasing, and the kilowatt-range tube can be realized. Therefore, the dynamic magnification radiography is possible using a flat panel detector with a pixel size of less than 100 μm.

## ACKNOWLEDGMENTS

This work was supported by Grants-in-Aid for Scientific Research (13470154, 13877114, 16591181, and 16591222) and Advanced Medical Scientific Research from MECSST, Health and Labor Sciences Research Grants (RAMT-nano-001, RHGTEFB-genome-005 and RHGTEFB-saisei-003), Grants from the Keiryo Research Foundation, The Promotion and Mutual Aid Corporation for Private Schools of Japan, Japan Science and Technology Agency (JST), and the New Energy and Industrial Technology Development Organization (NEDO, Industrial Technology Research Grant Program in '03).

## REFERENCES

1. R. Germer, "X-ray flash techniques," *J. Phys. E: Sci. Instrum.*, **12**, 336-350, 1979.
2. E. Sato, Y. Hayasi, R. Germer, E. Tanaka, H. Mori, T. Kawai, T. Ichimaru, S. Sato, K. Takayama and H. Ido, "Portable x-ray generator utilizing a cerium-target radiation tube for angiography," *J. Electron Spectrosc. .Related Phenom.*, **137-140**, 699-704, 2004.
3. E. Sato, E. Tanaka, H. Mori, T. Kawai, T. Ichimaru, S. Sato, K. Takayama and H. Ido, "Demonstration of enhanced K-edge angiography using a cerium target x-ray generator," *Med. Phys*, **31**, 3017-3021, 2004.
4. E. Sato, S. Kimura, S. Kawasaki, H. Isobe, K. Takahashi, Y. Tamakawa and T. Yanagisawa, "Repetitive flash x-ray generator utilizing a simple diode with a new type of energy-selective function," *Rev. Sci. Instrum.*, **61**, 2343-2348, 1990.
5. A. Shikoda, E. Sato, M. Sagae, T. Oizumi, Y. Tamakawa and T. Yanagisawa, "Repetitive flash x-ray generator having a high-durability diode driven by a two-cable-type line pulser," *Rev. Sci. Instrum.*, **65**, 850-856, 1994.
6. E. Sato, K. Takahashi, M. Sagae, S. Kimura, T. Oizumi, Y. Hayasi, Y. Tamakawa and T. Yanagisawa, "Sub-kilohertz flash x-ray generator utilizing a glass-enclosed cold-cathode triode," *Med. & Biol. Eng. & Comput.*, **32**, 289-294, 1994.
7. K. Takahashi, E. Sato, M. Sagae, T. Oizumi, Y. Tamakawa and T. Yanagisawa, "Fundamental study on a long-duration flash x-ray generator with a surface-discharge triode," *Jpn. J. Appl. Phys.*, **33**, 4146-4151, 1994.
8. E. Sato, Y. Hayasi, R. Germer, E. Tanaka, H. Mori, T. Kawai, T. Ichimaru, K. Takayama and H. Ido, "Quasi-monochromatic flash x-ray generator utilizing weakly ionized linear copper plasma," *Rev. Sci. Instrum.*, **74**, 5236-5240, 2003.
9. E. Sato, Y. Hayasi, R. Germer, E. Tanaka, H. Mori, T. Kawai, T. Ichimaru, S. Sato, K. Takayama and H. Ido, "Sharp characteristic x-ray irradiation from weakly ionized linear plasma," *J. Electron Spectrosc. Related Phenom.*, **137-140**, 713-720, 2004.
10. E. Sato, E. Tanaka, H. Mori, T. Kawai,S. Sato and K. Takayama, "Clean monochromatic x-ray irradiation from weakly ionized linear copper plasma," *Opt. Eng.*, **44**, 049002-1-6, 2005.
11. E. Sato, M. Sagae, E. Tanaka, Y. Hayasi, R. Germer, H. Mori, T. Kawai, T. Ichimaru, S. Sato, K. Takayama and H. Ido: Quasi-monochromatic flash x-ray generator utilizing a disk-cathode molybdenum tube, *Jpn. J. Appl. Phys.*, **43**, 7324-7328, 2004.

12. E. Sato, E. Tanaka, H. Mori, T. Kawai, T. Ichimaru, S. Sato, K. Takayama and H. Ido, "Compact monochromatic flash x-ray generator utilizing a disk-cathode molybdenum tube," *Med. Phys.*, **32**, 49-54, 2005.
13. A. Momose, T. Takeda, Y. Itai and K. Hirano, "Phase-contrast x-ray computed tomography for observing biological soft tissues," *Nature Medicine*, **2**, 473-475, 1996.
14. M. Ando, A. Maksimenko, H. Sugiyama, W. Pattanasiriwisawa, K. Hyodo and C. Uyama, "A simple x-ray dark- and bright- field imaging using achromatic Laue optics, *Jpn. J. Appl. Phys.*, **41**, L1016-L1018, 2002.
15. H. Mori, K. Hyodo, E. Tanaka, M. U. Mohammed, A. Yamakawa, Y. Shinozaki, H. Nakazawa, Y. Tanaka, T. Sekka, Y. Iwata, S. Honda, K. Umetani, H. Ueki, T. Yokoyama, K. Tanioka, M. Kubota, H. Hosaka, N. Ishizawa and M. Ando, "Small-vessel radiography in situ with monochromatic synchrotoron radiation," *Radiology*, **201**, 173-177, 1996.
16. K. Hyodo, M. Ando, Y. Oku, S. Yamamoto, T. Takeda, Y. Itai, S. Ohtsuka, Y. Sugishita and J. Tada, "Development of a two-dimensional imaging system for clinical applications of intravenous coronary angiography using intense synchrotron radiation produced by a multipole wiggler," *J. Synchrotron Rad.*, **5**, 1123-1126, 1998.
17. E. Sato, K. Sato, T. Usuki and Y. Tamakawa, "Film-less computed radiography system for high-speed imaging," *Ann. Rep. Iwate Med. Univ. Sch. Lib. Arts and Sci.*, **35**, 13-23, 2000.
18. A. Ishisaka, H. Ohara and C. Honda, "A new method of analyzing edge effect in phase contrast imaging with incoherent x-rays," *Opt. Rev.*, **7**, 566-572, 2000.
19. E. Sato, Y. Hayasi, R. Germer, E. Tanaka, H. Mori, T. Kawai, T. Ichimaru, S. Sato, K. Takayama and H. Ido, "Portable x-ray generator utilizing a cerium-target radiation tube for angiography," *J. Electron Spectrosc. Related Phenom.*, **137-140**, 699-704, 2004.
20. E. Sato, E. Tanaka, H. Mori, T. Kawai, T. Ichimaru, S. Sato, K. Takayama and H. Ido, "Demonstration of enhanced K-edge angiography using a cerium target x-ray generator," *Med. Phys*, **31**, 3017-3021, 2004.
*dresato@iwate-med.ac.jp; phone +81-19-651-5111; fax +81-19-654-9282